REVISTA MATÉRIA V.20 N.02

ISSN 1517-7076 artigo 11610, pp.420-435, 2015

Corrosion protection in sulfate medium by self-assemb films adsorbed on AA 2024 T3 aluminum alloy surface

Aline Viomar[1], Maysa Terada[2], Isolda Costa[2],
Paulo Rogério Pinto Rodrigues[1], Claudia Schlindwein[1],
Everson do Prado Banczek[1]

[1]Universidade Estadual do Centro-Oeste/ Departamento de Química/Unicentro. Guarapuava-PR, Brazil
email: prprodrigues@gmail.com; claudia_schlindwein@hotmail.com; edopradobanczek@yahoo.com.br
[2]IPEN/CNEN-SP/Centro de Ciências e Tecnologia de Materiais. Avenida Prof. Lineu Prestes 2242, São Paulo-SP, Brazil
email: maysaterada@uol.com.br; icosta@ipen.br

ABSTRACT

In this study, the corrosion protection provided by films of self-assembled molecules on the AA 2024-T3 aluminum alloy has been evaluated by electrochemical and non electrochemical techniques. The film was obtained by immersion of this alloy samples in a solution of 90 mg L^{-1} alkane-diphosphonate at 50 °C for 5 minutes. Chromating conversion treatment with trivalent or hexavalent chromium was carried out by immersion of AA 2024-T3 alloy samples for 2 minutes in a 20% (v/v) solution of 650 Chromical TCP (SurTec) at 40 °C. Electrochemical characterization was performed by measurements of the open circuit potential (OCP), potentiodynamic polarization curves (PPC) and electrochemical impedance spectroscopy (EIS) in a solution of 0.5 mol L^{-1} sodium sulfate buffered with a solution of biphthalate potassium (0.1 mol L^{-1}) and sodium hydroxide (0.1 mol L^{-1}) as the electrolyte. SAM films obtained were analysed by infrared spectroscopy and SAM was found in surface. Surface observation by scanning electron microscopy (SEM) showed that the trivalent chromium layers ere deposited on metal surface. The results show that the surface treatment with self-assembled molecules provides protection against corrosion of the AA 2024-T3 aluminum alloy.

Keywords: AA 2024-T3, corrosion, trivalent chromium.

1. INTRODUCTION

Interactions between molecules and surfaces are frequently studied aspects in the area of modern surface science. These interactions are highly dependent on the chemical nature of the molecules and range from weak, as observed, for example, in n-alkane adsorbed on gold or graphite [1], to interactions that are strong enough to break chemical bonds within the molecule itself, for example, ethylene on platinum [2]. A molecule-substrate interaction of great relevance is the spontaneous organization of atoms and molecules on a surface into ordered arrays, in particular, the spontaneous organization *(self-assembling)* of surfactant molecules adsorbed on the surface of a transition metal. The number of Investigations with self-assembling molecules has rapidly increased, due to the ability of these structures to modify the chemical and physical properties of surfaces.

The notion of organized molecules or highly ordered structures is not new [3]; examples of ordered atoms and molecules have been shown in biology, chemistry and physics. In the context of surface chemistry, however, it is important to mention that amphiphilic molecules, spontaneously organized and assembled on metal surfaces, are only sub-points of semi-organized films that have been reported and characterized. Amphiphilic molecules can organize themselves on a variety of interfaces, such as liquid-liquid, liquid-air, liquid-solid and solid-air interfaces [4].

Self-Assembling Molecules (SAM) have been described [5, 6] as molecular aggregates organized with a specific affinity for metal surfaces, interacting with the surface by adsorption. Historically, the use of self-assembling molecules on solid electrodes was firstly described by Sagiv and Maoz *et al.* [7] that produced organized monolayers via a silanization process. These authors demonstrated that alkyl-trichlorosilane on

Autor Responsável: Everson do Prado Banczek Data de envio: 27/10/2014 Data de aceite: 18/03/2015

10.1590/S1517-707620150002.0043

polar surfaces, for example, those with hydroxyl groups, leads to the formation of organized monolayers chemically bound to the surface. Since then, silanization has been widely used as a means of electrode surface modification. Thus, it has become common to combine the Sagiv approach with silanization procedures for assembling monolayers organized on different active surfaces, such as SnO_2 or Al_2O_3, and numerous studies have adopted this method [8, 9].

The use of self-assembled layers has grown steadily over the past years [10,11]. While a wide variety of functionalized alkanes and metal surfaces have been examined, the most commonly used and studied system is undoubtedly thiols on gold surfaces [12,13]. The last decade, the SAM use as corrosion inhibitors has been proposed [14-19-22].

Surface treatments with self-assembling molecules for corrosion protection of aluminum and its alloys have also been evaluated as potential replacements for hexavalent chromium in chromating processes [19, 23]. The purpose of these studies was to evaluate whether the surface layer formed can inhibit corrosion by acting as a physical barrier between the aggressive medium and the metal surface. In particular, for aluminum or aluminum alloys, the self-assembling molecules used are based on alkane-diphosphonates. It is known that alkane-diphosphonates have high affinity for aluminum oxide; however, the interaction between the oxide and the self-assembling molecules is not always strong enough to resist corrosion reaction products.

In this context, this study aims to evaluate the effect of self-assembled molecules on the corrosion protection of the AA 2024-T3 alloy and to compare the results with those obtained from chromate conversion coatings obtained in solutions with trivalent chromium.

2. METHODS AND MATERIALS

2.1. Preparation of the AA 2024-T3 aluminum samples

The surface of the AA 2024-T3 aluminum alloy investigated in this study was prepared by grinding with SiC emery paper, sequentially from #600 to #1200, followed by degreasing with ethanol in a sonicator, rinsing with water and drying under a hot air stream. The composition of the investigated alloy is shown in Table 1.

Table 1: Chemical composition (wt.%) of the aluminum alloy AA 2024-T3.

Fe	Cu	Mn	Si	Sn*	Zn*
0.163	4.060	0.626	0.106	<0.183	195.71

(*) – concentration in ppm

2.2. Obtaining self-assembled films

Surface treatment of the AA 2024-T3 alloy with self-assembling molecules was carried out by immersing the alloy in an aqueous solution of 90 mg L^{-1} alkane-diphosphonate $[PO(OH)_2\text{-}(CH_2)_n\text{-}PO(OH)_2]$ (X Gardobond 4661), at (50 ± 2) °C for 5 minutes.

2.3. Conversion coating treatment with solution of trivalent or hexavalent chromium

Chromating conversion treatment with trivalent chromium was carried out by immersion of AA 2024-T3 alloy samples for 2 minutes in a 20% (v/v) solution of 650 Chromical TCP (SurTec) at 40 °C, followed by drying under a hot air stream. Conversion coating with hexavalent chromium film was also performed by immersion of the aluminum alloy samples for 3 minutes in a 20 g/L solution of 653 Chromical TCP (SurTec) at 40 °C, also followed by drying under a hot air stream.

2.4. Electrochemical characterization

Electrochemical characterization of the untreated and surface treated aluminum alloy samples was accomplished by exposure of a surface area corresponding to 1 cm^2. The electrochemical tests were carried out in a naturally aerated 0.5 mol L^{-1} Na_2SO_4 solution with pH adjusted to 4.0 with a buffer solution of 0.1 mol L^{-1} potassium biphthalate and 0.1 mol L^{-1} sodium hydroxide at 20 °C.

A three-electrode experimental set-up was used with a platinum wire as the counter electrode, a mercurous sulfate electrode Hg/Hg_2SO_4 (MSE) as the reference electrode and an electrode prepared with the

AA 2024-T3 aluminum alloy as the working electrode. The electrochemical tests used for corrosion evaluation of the untreated or surface treated samples were open circuit potential measurements as a function of time, electrochemical impedance spectroscopy (EIS) and potentiodynamic anodic polarization. EIS measurements were performed using a frequency response analyzer (Gamry model EIS 300®) coupled to a Gamry PCI 4/300® potentiostat in the frequency range from 10 kHz to 10 mHz, with a perturbation amplitude of 10 mV (rms) and a data acquisition rate of 10 points per decade. Anodic polarization curves were obtained with a scan rate of 1 mV s^{-1}.

2.5. Scanning electron microscopy

The aluminum alloy surface was observed by scanning electron microscopy (SEM) using a Philips XL30 microscope, prior to and after anodic polarization tests, to assess the effects of the surface treatments on the alloy corrosion resistance.

2.6. Infrared spectroscopy

Infrared (IR) spectra of the SAM powder, the 90 mg L^{-1} SAM solution, the SAM surface treated and the untreated AA2024 T3 alloy were obtained with a Nicolet IR 200 spectrophotometer.

3. RESULTS AND DISCUSSION

3.1. Infrared spectroscopy

Infrared spectra of the SAM powder and the SAM surface treated AA 2024-T3 alloy are shown in Figure 1.

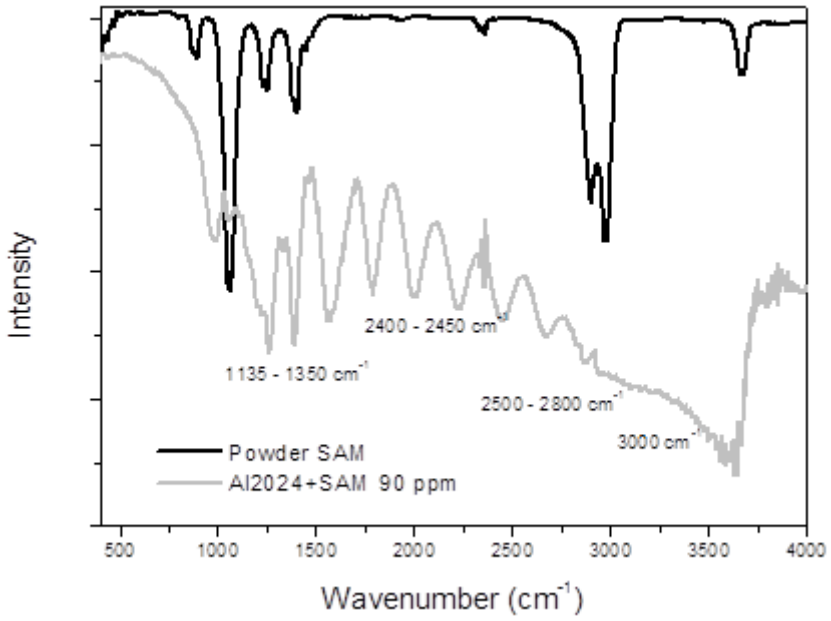

Figure 1: Infrared spectra of SAM powder and the AA 2024 T3 alloy surface treated in a solution with 90 mg L^{-1} SAM.

The infrared spectrum corresponding to the powder of the alkane-diphosphonate molecules used shows a band near 800 cm^{-1}, which is characteristic of the vibration of *ν*P-C [21] bonds, associated to phosphorus attached to the carbon present in the molecules. For higher wave numbers, between 1,135 and 1,350 cm^{-1}, there are three other bands related to the vibration of the υP=O [24] bond, and this vibration is characteristic of phosphonic compounds. Other bonds are present in these molecules and are characterized by vibrations in the regions of higher wave numbers, as in the case of vibration of the υP-H and νOH bonds, which have characteristic bands in the regions of 2,400-2,450 cm^{-1} and 2,575-2,800 cm^{-1} [24], respectively. In the spectrum presented in Figure 1, this band appears close to 2,500 cm^{-1}. The band observed at 3,000 cm^{-1} is characteristic of symmetrical and asymmetrical stretching of C-H bonds in saturated carbon chains.

Comparison of the spectrum of SAM as powder with that for the SAM treated surface, shows the same

vibration bands on either, solid or adsorbed SAM. SAM adsorbed on the surface of the AA 2024-T3 alloy is indicated by the spectral vibration bands of υP-C bonds at 800 cm^{-1} and that of υP=O at 1,135-1,350 cm^{-1}. These bands for the SAM surface treated samples are less strong, indicating that the adsorption of SAM on the aluminum alloy changes the vibration array of these molecules.

3.2. Scanning electron microscopy

Scanning electron microscopy (SEM) analysis and energy dispersive spectroscopy (EDS) measurements were accomplished at different regions of the aluminum alloy surface and the results are presented in Figure 2. A large number of precipitates can be observed, mainly the Mn-rich and Mg-rich ones, containing Al, Fe and Cu in their compositions.

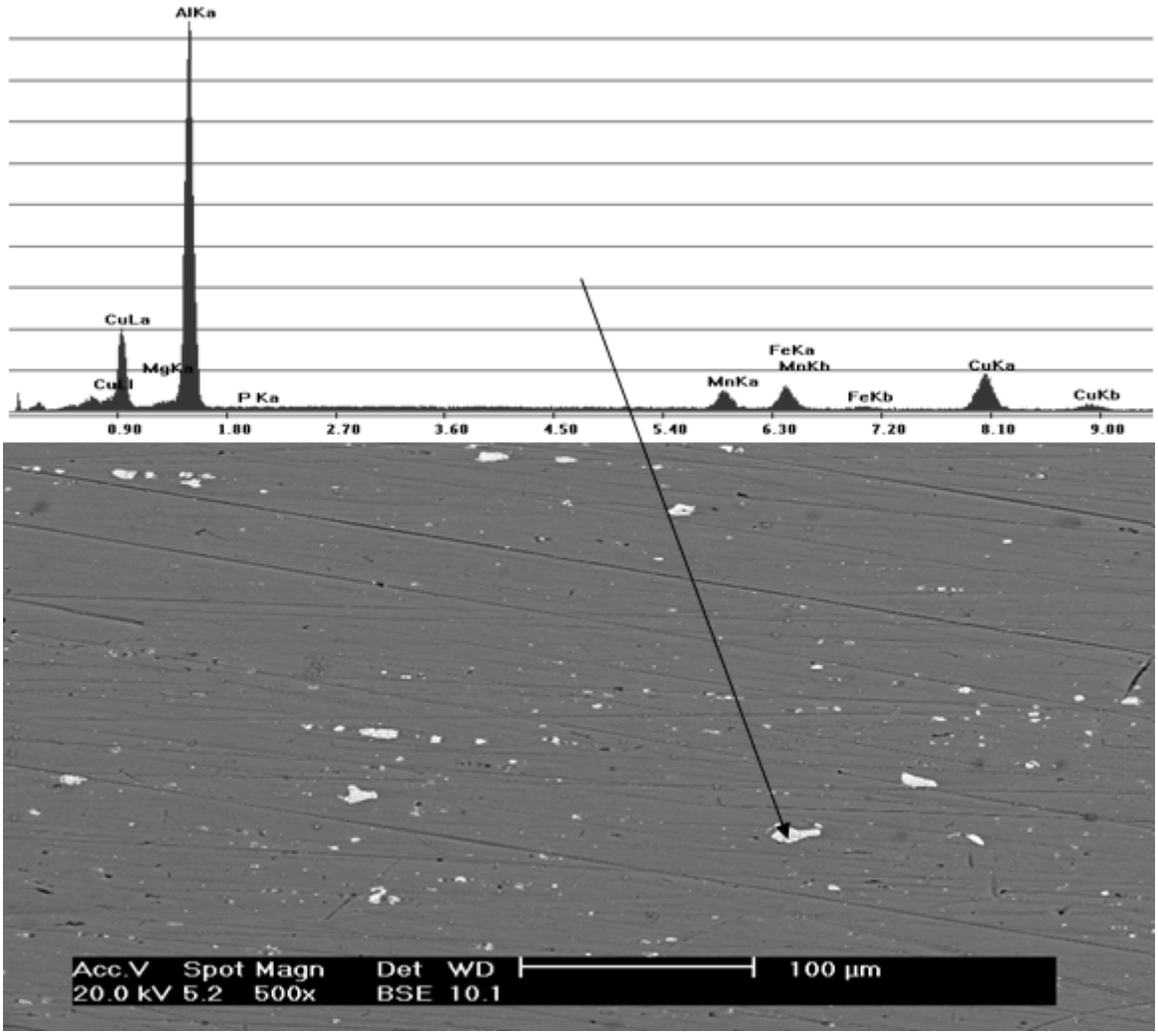

Figure 2: SEM micrograph and EDS spectrum of the AA 2024-T3 alloy surface. EDS was obtained on a Mn-rich precipitate.

The surface of the SAM-treated AA 2024-T3 alloy was also evaluated by scanning electron microscopy, as Figure 3 shows. Corrosion attack is observed mainly associated to small Mg-rich precipitates which are more active than the aluminum alloy matrix. The attack is favored in the SAM solution used which is acid (pH = 3.2) and corrosive for the surface at the more susceptible areas.

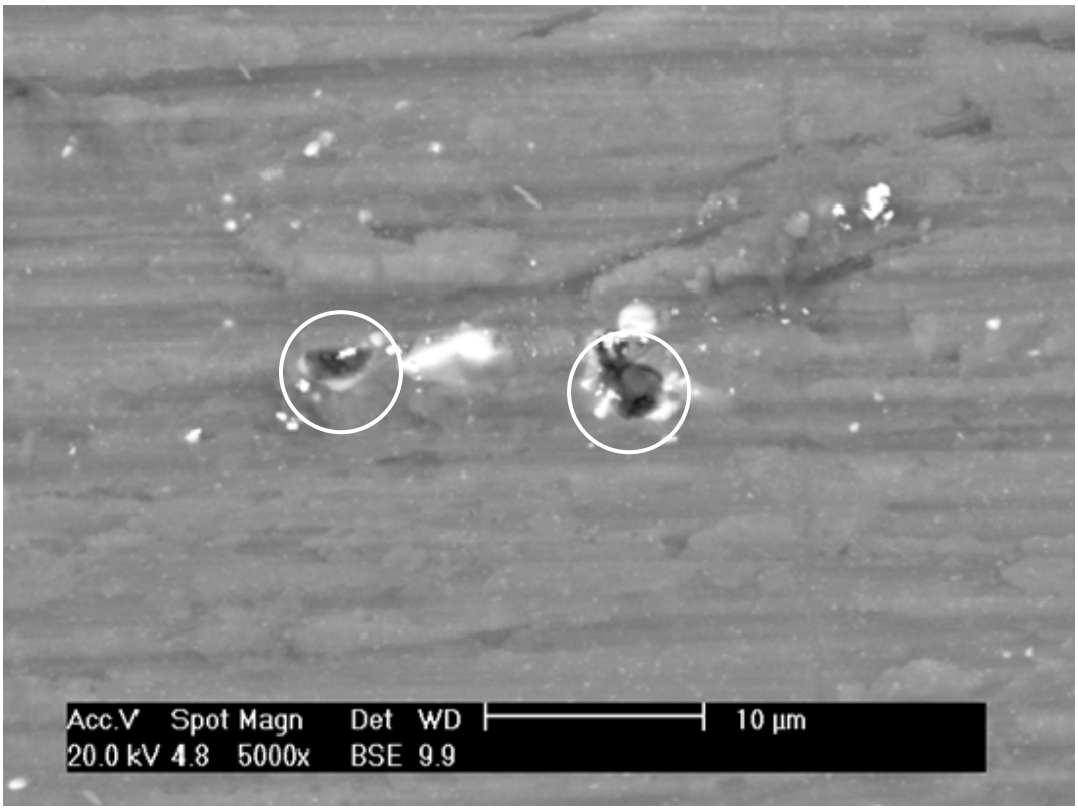

Figure 3: Micrograph of the AA 2024-T3 alloy surface treated with SAM.

SAM was identified on the AA 2024-T3 surface, as Figure 4 shows; as clusters, corresponding to the darker areas, showing a heterogeneous distribution on the surface. A peak corresponding to phosphorus is seen associated to the SAM molecules, whose molecular formula is of the type $[PO(OH)_2\text{-}(CH_{2)n\text{-}}PO(OH)_2]$.

The surfaces of the AA 2024-T3 alloy, treated with either trivalent or hexavalent chromium conversion coating were also observed by SEM and analyzed by EDS, and the results are shown in Figures 5 (a) and (b), respectively. The surface films formed on both types of solution shows despite of being very thin (order of nanometers) impairing their analysis by EDS [25].

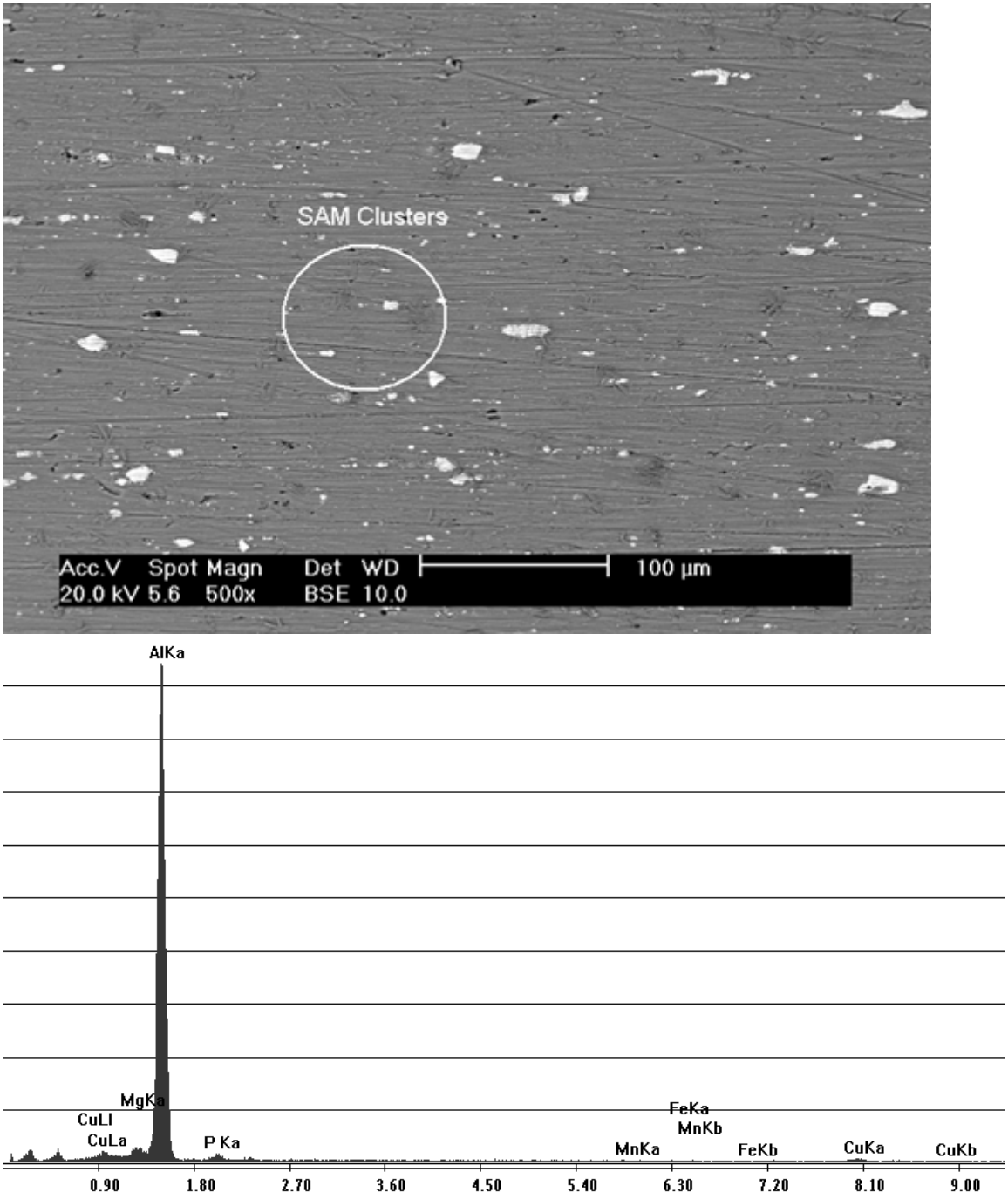

Figure 4: Micrograph and EDS spectrum of the AA 2024-T3 alloy treated with SAM.

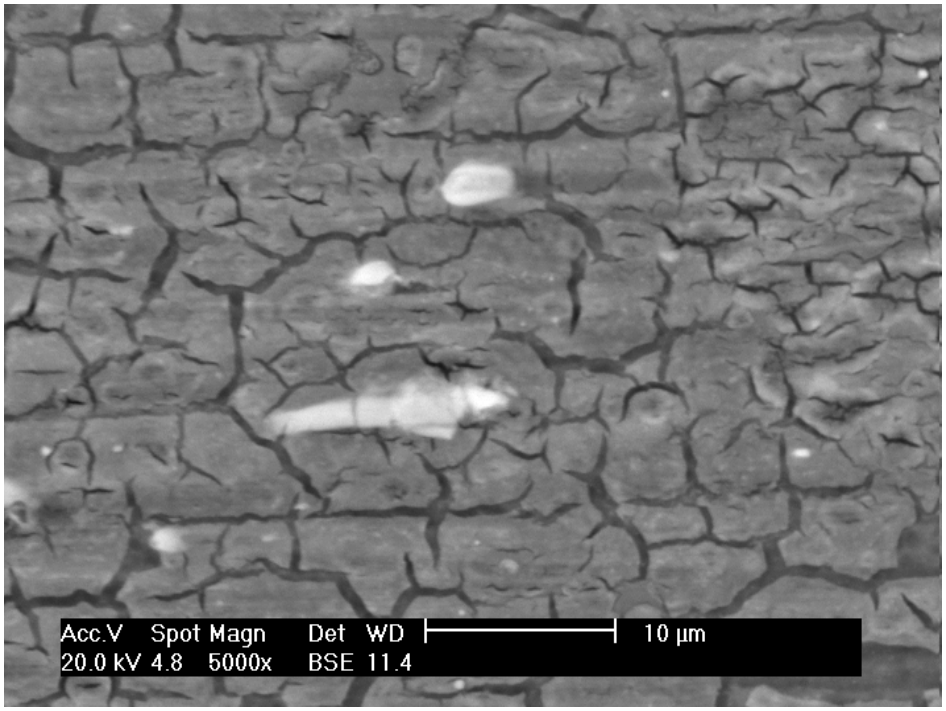

(a)

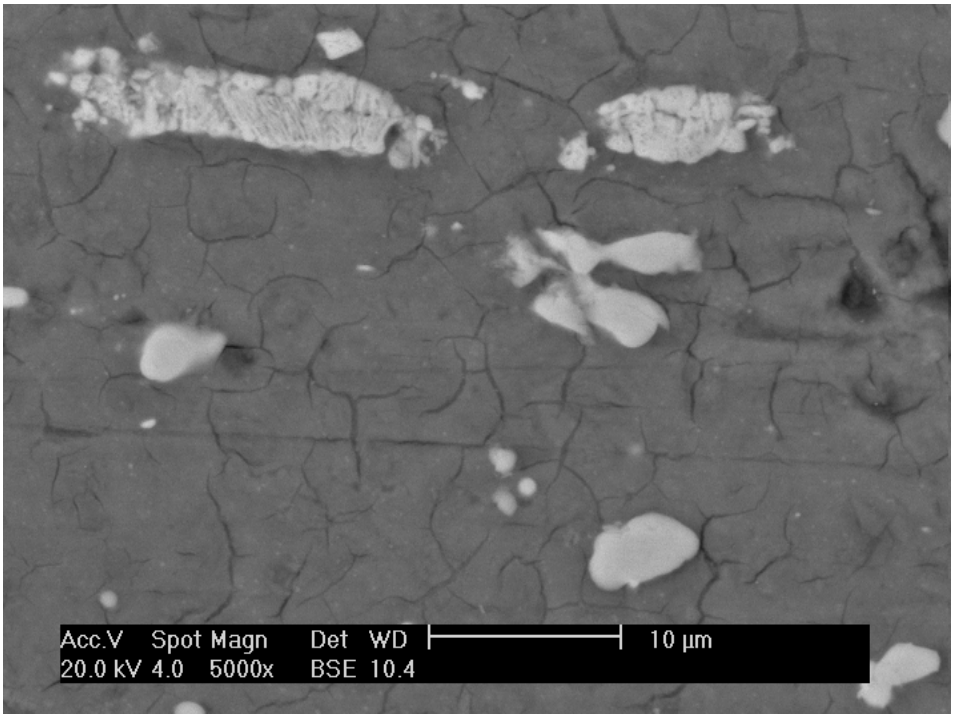

(b)

Figure 5: Micrographs of the AA 2024-T3 alloy treated with (a) trivalent chromium and (b) hexavalent chromium.

3.3. Electrochemical results for SAM surface treated samples

Figure 6 shows the open circuit potential as a function of immersion time in a solution of 0.5 mol L^{-1} Na_2SO_4,

pH = 4.0, for untreated and SAM treated samples. The open circuit potential increases with immersion time; however, a larger period of time is required for potential stabilization of SAM treated samples than for the untreated ones. Much higher stable potentials were obtained for the SAM treated alloy, as compared to the untreated samples. The corrosive character of the SAM solution towards the aluminum alloy leading to attack of active precipitates at the surface and, eventually, their detachment, must explain this result. It was observed that for aluminum sample SAM coated potential shifts to more positive values suggesting a higher corrosion resistance of the material with SAM.

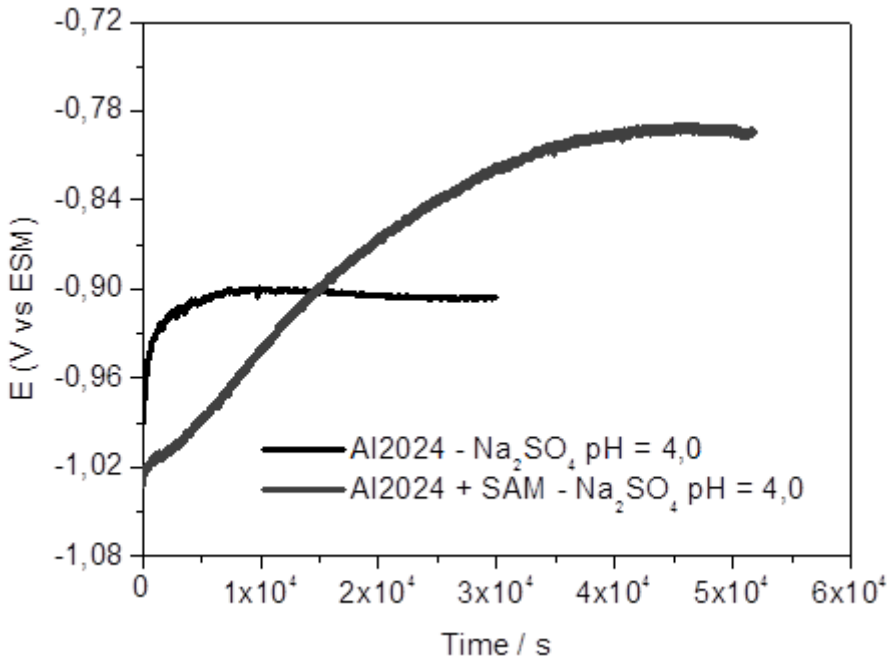

Figure 6: Open circuit potential as a function of time of immersion of the AA 2024-T3 alloy in 0.5 mol L^{-1} Na_2SO_4, pH = 4.0.

Electrochemical impedance spectroscopy (EIS) measurements, performed after potential stabilization, are shown in Figure 7 for the untreated and SAM-treated samples. Nyquist diagrams show flattened capacitive arcs for both types of surfaces but the SAM treatment led to higher impedances comparatively to the untreated one. A clear separation of two time constants is indicated in the Bode phase angle diagrams of the treated samples, whereas the presence of a shoulder is suggested in the diagram of the untreated ones. It is proposed that the time constant at higher frequencies is due to the aluminum oxide film, whereas that between 10 and 1 Hz, is due to charge transfer processes in parallel with the charging of the double layer.

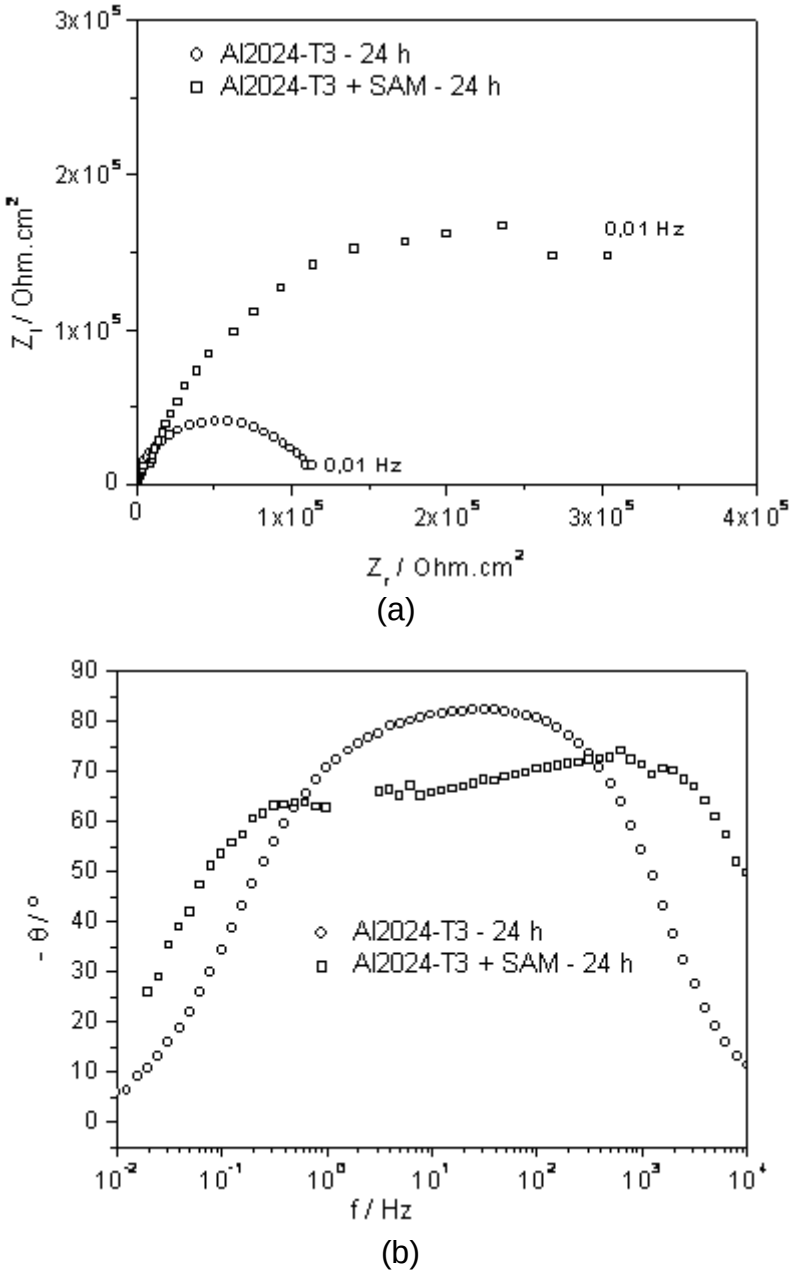

Figure 7: (a) Nyquist and (b) Bode phase angle diagrams for untreated and SAM-treated AA 2024-T3 alloy in 0.5 mol L^{-1} Na_2SO_4 solution, pH=4.0.

Although aluminum oxide obtained by anodizing has a duplex character, consisting of an inner compact layer and an outer porous layer [26], and their individual contributions being identified by EIS tests, it is very difficult to separate the contribution of each individual layer by EIS of very thin alumina films, such as those formed under the conditions adopted in this work.

For the SAM-treated aluminum alloy the two time-constants are clearly separated and the results suggest a more protective surface film and charge transfer processes with slower kinetics.

3.3.2. Surface treatment with trivalent chromium

Figure 8 shows the EIS diagrams for the AA 2024-T3 alloy after surface treatment with trivalent chromium. The Nyquist diagrams show one capacitive arc and high impedance values (order of 10^6 Ohm.cm^2) suggesting the presence of a highly protective passive film. The diagrams were fairly stable from 24 to 144 hours of immersion, indicating the high stability of this film on the aluminum alloy in the test solution used.

The Bode phase angle diagrams suggest at least two time constants with that at frequencies in the

range from 10 to 1 kHz related to the chromate layer; whereas that at frequencies from 10 to 1 Hz is associated with charge transfer processes. It is noteworthy that the time constant at lower frequencies shifts to lower frequencies and the related phase angles to higher values with increasing immersion time, indicating an improvement in protection of the aluminum alloy as time in the sulphate solution progresses, likely due to the precipitation of corrosion products on the defects of the chromate layer.

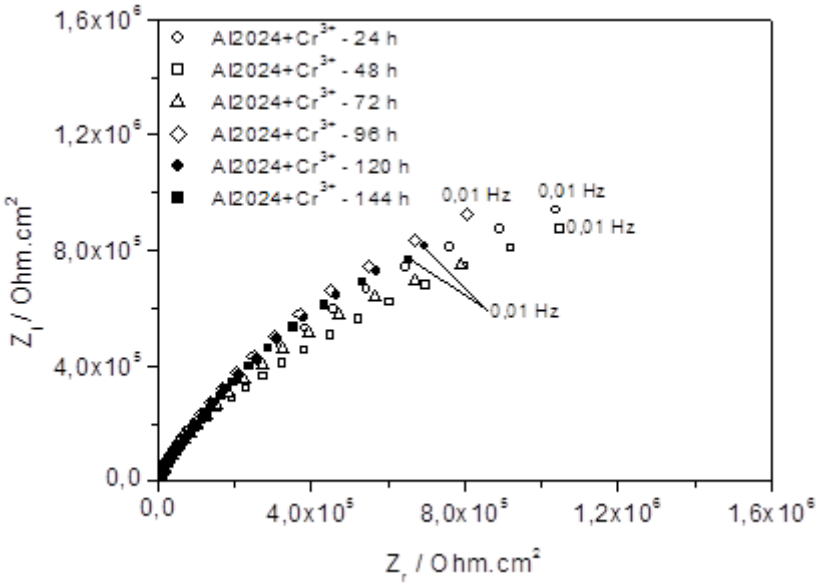

(a)

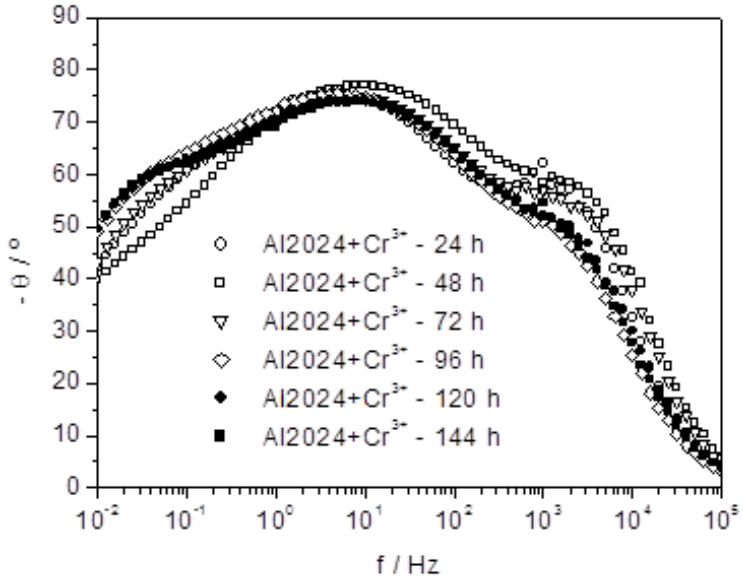

(b)

Figure 8: Impedance diagrams for AA 2024-T3 alloy in 0.5 mol L-1 Na_2SO_4 solution, pH = 4.0, treated in solution with trivalent chromium: (a) Nyquist and (b) Bode phase angle diagram.

3.3. Anodic polarization curves

Figure 9 compares the potentiodynamic anodic polarization curves for untreated and SAM-treated samples. Lower current densities and a shift in the corrosion potential to more positive values, were associated to the SAM-treated samples. Although SAM adsorption usually leads to polarization of the cathodic reaction by hindering the access of oxygen into the metallic interface, this results shows that polarization of the anodic reaction also occurs. This must be related to the attack and removal of precipitates which are more active than the matrix leading to a “cleaner” surface. Passive film breakdown for the SAM-treated sample also

occurred at nobler potentials (-0.490 V_{MSE}) than for the untreated alloy two breakdown potentials were observed, being the first one at 1.2 V_{MSE} and after repassivation on -0.790 and second V_{MSE}, suggesting that the oxide is less stable in the absence of SAM. Besides, after the passive film breakdown, lower current densities were associated with the samples treated with SAM. This result suggests that adsorbed molecules remained on the surface after localized passive film breakdown. The lower amount of precipitates on this type of sample is also responsible for the higher resistance to localized attack.

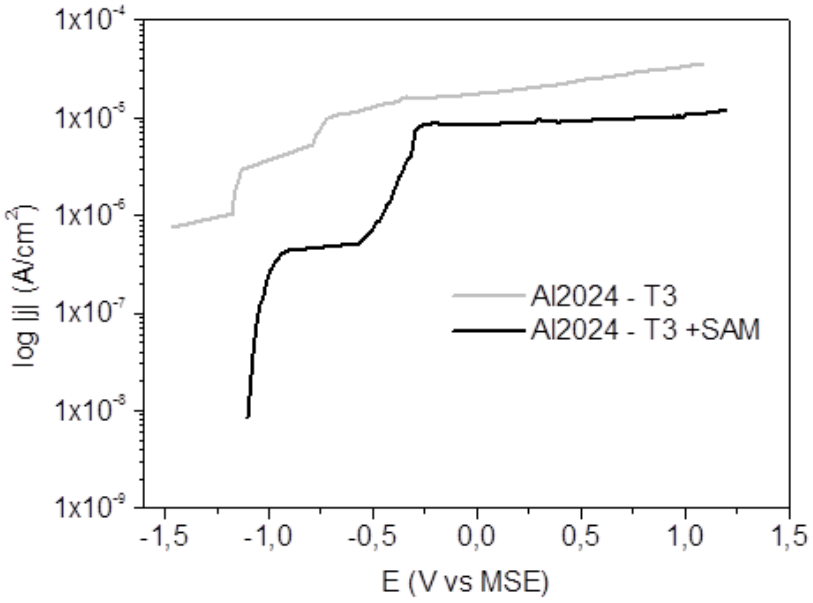

Figure 9: Potentiodynamic anodic polarization curves for untreated or SAM-treated AA2024-T3 alloy after 24 h or immersion in 0.5 mol L^{-1} Na_2SO_4 solution, pH = 4.0.

Figure 10 compares the anodic polarization curves of AA 2024-T3 treated with trivalent or hexavalent chromium ions. Very low current densities, typical of passive films were obtained for samples treated with hexavalente chromium, in the whole passive range, showing the higher resistance of the film formed by this treatment. Current densities typical of passive materials were obtained for both tested samples. However, rates obtained for Cr^{3+} were higher than those obtained for Cr^{6+} coating, suggesting that the latter promotes higher corrosion resistance to the aluminum alloy.

This behavior shows that the hexavalent chromium layer is more stable. The coating stability can be observed by the micrographs of Figure 13. It can be seen that the Cr^{3+} coating is more porous than Cr^{6+} plated. Additionally, it can be observed that the Cr^{3+} coating is more reactive because, after the anodic polarization that has been attacked and dissolved aluminum surface.

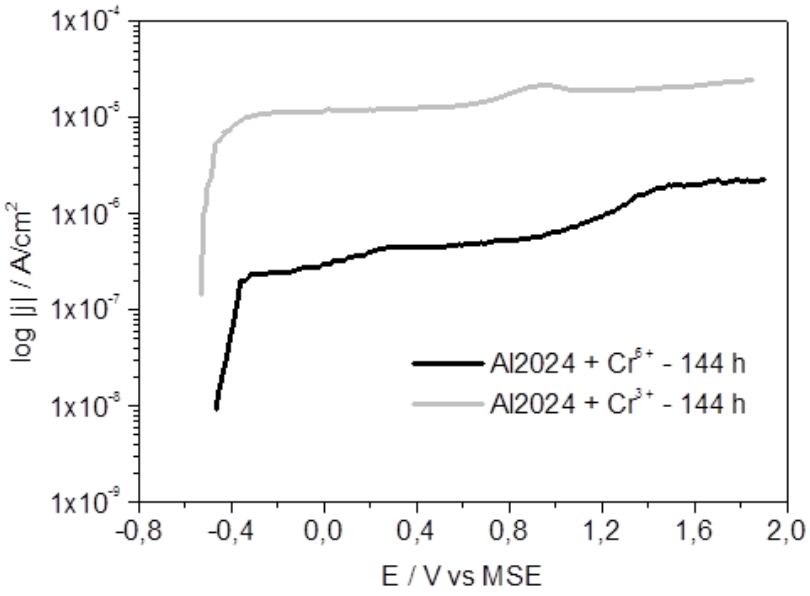

Figure 10: Anodic polarization curves of surface treated AA2024-T3 alloy in hexavalent or trivalent chromium ions in 0.5 mol L^{-1} Na_2SO_4 solution, pH=4.0.

3.4. Scanning electron microscopy after polarization tests

After polarization tests, the tested alloy surface was observed by SEM. Figure 11 shows the removal of small precipitates; mainly the Mg-rich types, but a large number of precipitates remain on the surface. The literature [27] reports the microstructural characteristics of the AA2024-T3 alloy, and the different activities of its precipitates.

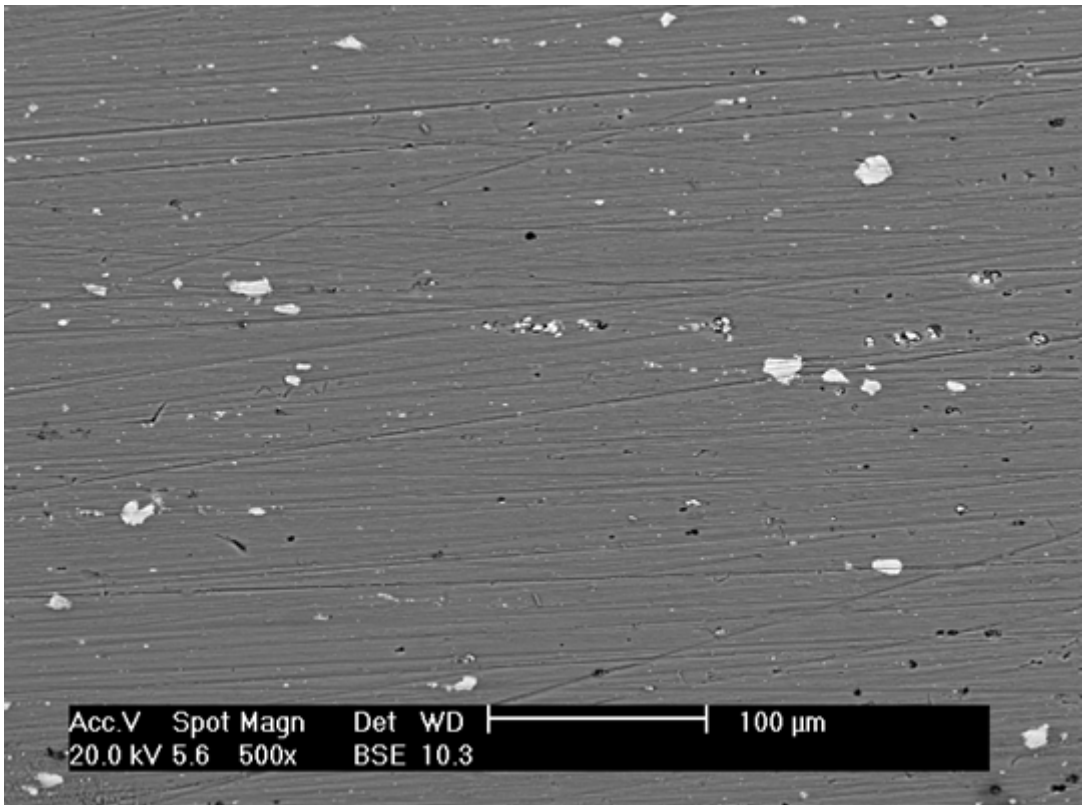

Figure 11: SEM micrograph of AA2024-T3 alloy surface after polarization in 0.5 mol L^{-1} Na_2SO_4 buffered solution (pH 4.0).

The surface of the SAM treated AA2024 alloy was also observed after polarization in 0.5 mol L^{-1} Na_2SO_4 solution, as Figure 12 shows. The detachment of a large number of small precipitates is observed but clusters of SAM are also seen on the surface after polarization, explaining the lower current densities after film breakdown, which was associated to this type of samples.

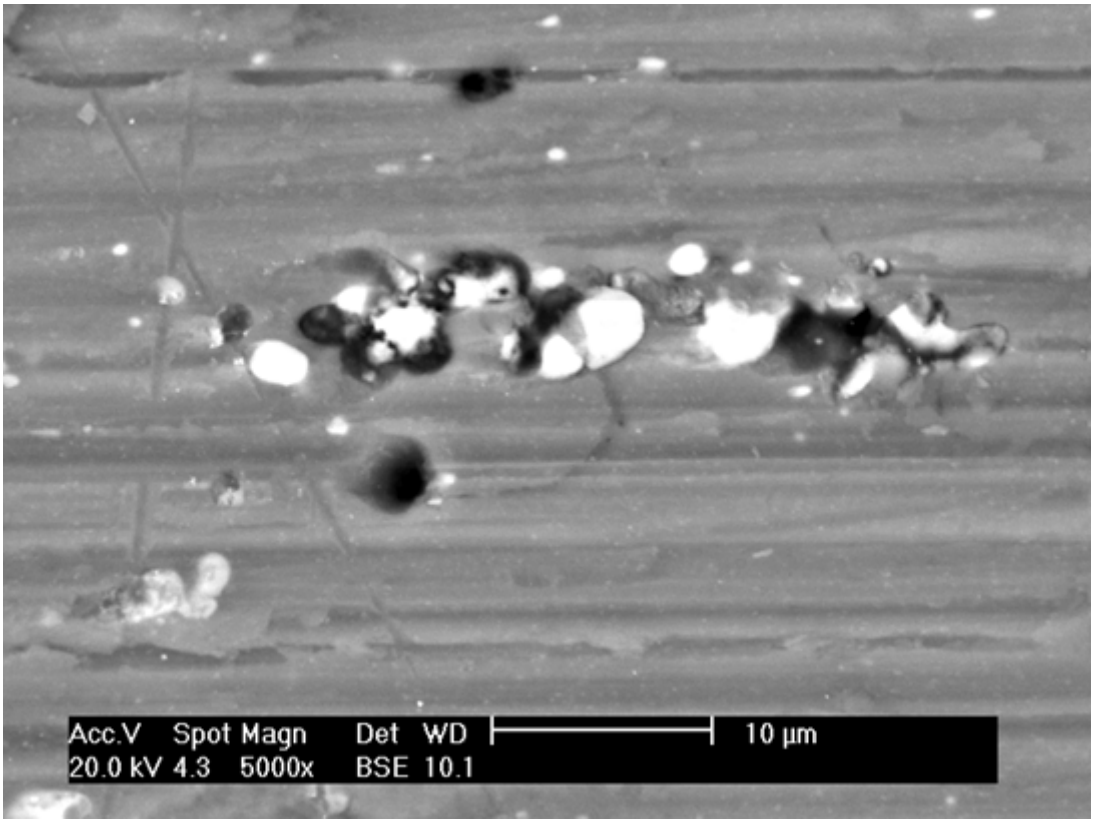

Figure 12: SEM micrograph of AA 2024-T3 alloy treated with SAM and polarized in 0.5 mol L^{-1} Na_2SO_4 solution (pH 4.0).

Figure 13 (a) and (b) show the surface treated with trivalent and hexavalent chromium, respectively, after polarization in sodium sulfate solution. The surface shows evidence of corrosive attack, increased roughness and the removal of the surface coating. However, hexavalent chromium coating was less attacked as compared to trivalent chromium, indicating that the former is more resistant to the corrosive medium. The comparison between Figures 13 (a) and 13 (b) with Figures 13 (c) and 13 (d) support these results.

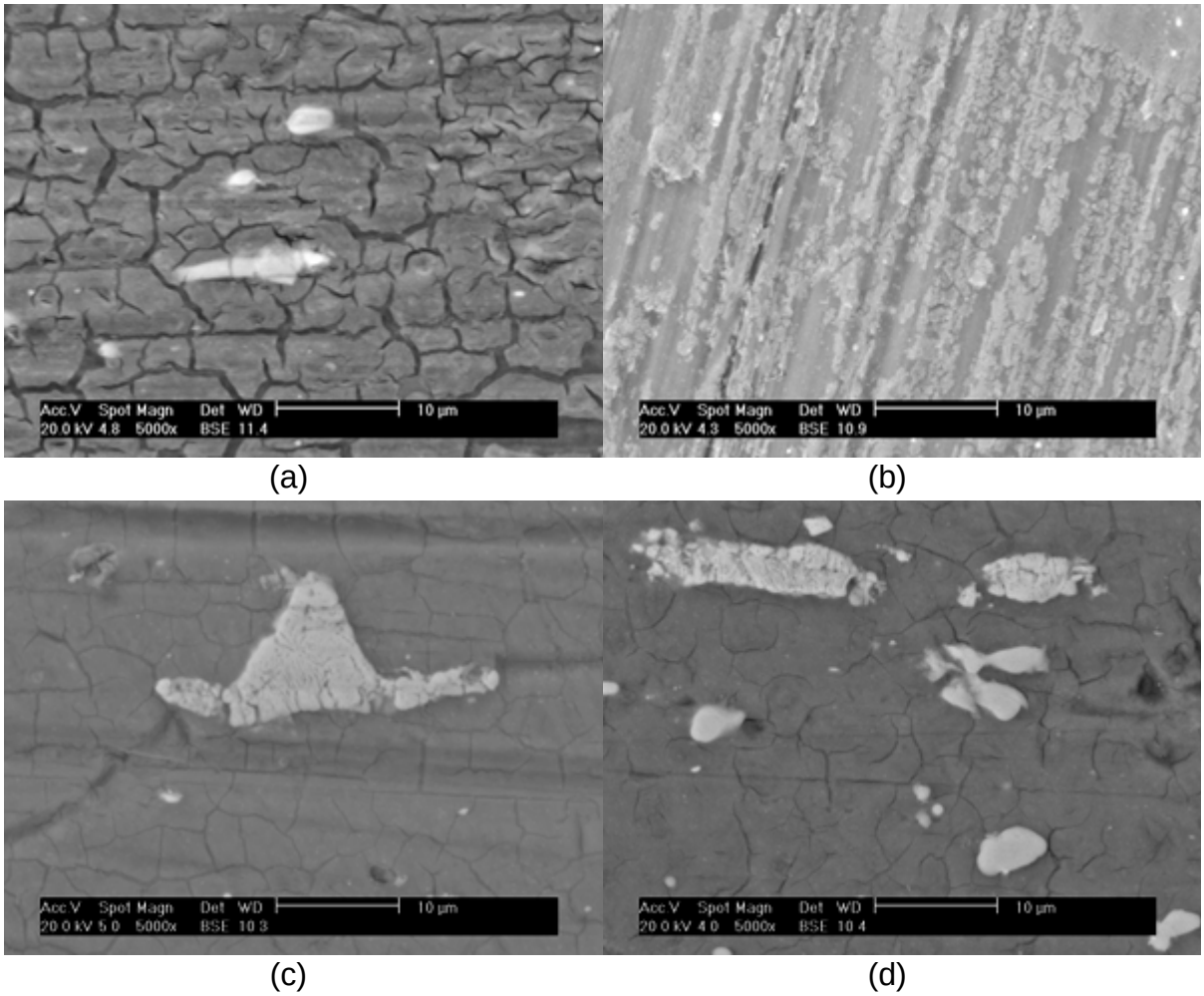

Figure 13: AA2024-T3 alloy treated with trivalent chromium (a) prior to and (b) after polarization and treated with hexavalent chromium (c) prior to and (d) after polarization in a 0.5 mol L^{-1} Na_2SO_4 solution.

4. CONCLUSIONS

From the results of infrared was possible to determine the presence of the SAM molecules on the aluminum surface, because characteristic bands were detected. The open circuit potential show the corrosive character of the SAM solution towards the aluminum alloy leading to attack of active precipitates at the surface and, eventually, their detachment, must explain this result. It was observed that for aluminum sample SAM coated potential shifts to more positive values suggesting a higher corrosion resistance of the material with SAM.

The treatment of the AA 2024-T3 alloy with self-assembling molecules (SAM) resulted in a surface with higher impedances and associated to lower current densities compared to the untreated alloy. Nevertheless, the molecules are not uniformly distributed on the surface but are strongly attached to the surface remaining on it after polarization. The conversion coating treatment with trivalent chromium resulted in a surface with high corrosion resistance.

5. ACKNOWLEDGEMENT

The authors are thankful to CNP_q for the financial support.

6. BIBLIOGRAPHY

[1] GIANCARLO, L.C., FILYNN, G.W., “Scanning tunneling and atomic-force microscopy probes of self-assembled, physisorbed monolayers - peeking at the peaks”, *Annual Review Physical Chemistry*, v. 49, pp. 297, 1998.

[2] KESMODEL, L.L., DUBOIS, L.H., SOMORJAI, G.A., “Dynamical LEED study of C_2H_2 and C_2H_4 chemisorption on Pt(111): evidence for the ethylidyne group”, *Chemical Physics Letters*, v. 56, n. 2, pp.

267-271, 1978.

[3] WHITESIDES, G, M, GRZYBOWSKI, B, A, "Self-assembly at all scales", *Science*, v. 295, n. 5564, pp. 2418-2421, 2002.

[4] SMITH, R.K., LEWIS, P.A., WEISS, P.S., "Patterning self-assembled monolayers", *Progress in Surface Science*, v. 75, pp. 1-68, n.1-2, 2004.

[5] FREIRE, R.S., PESSOA, C.A., KUBOTA, L.T., "Self-assembled monolayers applications for the development of electrochemical sensors", *Química Nova*, v. 26, n. 3, pp. 381-389, 2003.

[6] SCHREIBER, F., "Structure and growth of self-assembling monolayers" *Progress in Surface Science*, v. 65, n. 5-8, pp. 151-257, 2000.

[7] MAOZ, R., SAGIV, J., "On the formation and structure of self-assembling monolayers. I. A comparative atr-wettability study of Langmuir—Blodgett and adsorbed films on flat substrates and glass microbeads", *Journal of Colloid and Interface Science*, v. 100, n. 2, pp. 465-496, 1984.

[8] BRITT, D.W., HLADY, W., "An AFM study of the effects of silanization temperature, hydration, and annealing on the nucleation and aggregation of condensed ots domains on mica", *Journal of Colloid Interface Science*, v. 178, n. 2, pp. 775-784, 1996.

[9] HATTON, R.A., DAY, R.S., CHESTERS, M.A., WILLIS, M.R.," Organic electroluminescent devices: enhanced carrier injection using an organosilane self assembled monolayer (SAM) derivatized ITO electrode", *Thin Solid Films*, v. 394, n. 1-2, pp. 291-296, 2001.

[10] ULMAN, A., *Ultrathin Organic Films*, Academic Press, New York, 1991.

[11] WINK, T., VAN ZUILEN, S.J., BULT, A., et al., "Self-assembled monolayers for biosensors", *Analyst*, v. 122, n. 4, pp. 43R-53R, 1997.

[12] CHAKI, N, K, VIJAYAMOHANAN, K, "Self-assembled monolayers as a tunable platform for biosensor applications", *Biosensors and Bioelectronics*, v. 17, n.1-2, pp. 1-12, 2002.

[13] GOODING, J.J., HIBBERT, D.B., "The application of alkanethiol self assembled monolayers to enzyme electrodes", *Trends in Analytical Chemistry*, v. 18, n.10, pp. 525-533, 1999.

[14] ARAMAKI, K., SHIMURA, T., "Preparation of a one-dimensional polymer film on passivated iron by modification of a carboxylate ion self-assembled monolayer with octyltriethoxysilane for preventing passive film breakdown", *Corrosion Science*, v. 46, n.10, pp. 2533-2548, 2004.

[15] TELEGDI, J., RIGÓ, T., KÁLMÁN, E., "Molecular layers of hydroxamic acids in copper corrosion inhibition", *Journal of Electroanalytical Chemistry*, v. 582, n. 1-2, pp. 191-201, 2005.

[16] HINTZE, P.E., CALLE, L.M., "Electrochemical properties and corrosion protection of organosilane self-assembled monolayers on aluminum 2024-T3", *Electrochimica Acta*, v. 51, n. 8-9, pp. 1761-1766, 2006.

[17] FELHOSI, I., TELEGDI, J., PALINKAS, G., KALMAN, E.," Kinetics of self-assembled layer formation on iron", *Electrochimica Acta*, v .47, n.13-14, pp. 2335-2340, 2002.

[18] NOZAWA, K., NISHIARA, H., ARAMAKI, K., "Chemical modification of alkanethiol monolayers for protecting iron against corrosion ", *Corrosion Science*, v. 39, n. 9, pp. 1625-1639, 1997.

[19] REIS, F.M., DE MELO, H.G., COSTA, I., "EIS investigation on Al 5052 alloy surface preparation for self-assembling monolayer", *Electrochimica Acta*, v. 51, n. 8-9, pp. 1780-1788, 2006.

[20] DALMORO, V., SANTOS, J.H.Z., ARMELIN E., et al., "A synergistic combination of tetraethylorthosilicate and multiphosphonic acid offers excellent corrosion protection to AA1100 aluminum alloy" , *Applied Surface Science*, n. 273, pp. 758– 768, 2013.

[21] DALMORO V., SANTOS, J.H.Z., ARMELIN, E., et al., "Phosphonic acid/silica-based films: A potential treatment for corrosion protection", *Corrosion Science*, n. 60, pp. 173–180, 2012.

[22] TRUEBA, M., TRASATTI P. S., "Pyrrole-based silane primer for corrosion protection of commercial Al alloys Part I: Synthesis and spectroscopic characterizationI", *Progress in Organic Coatings*, n. 66, pp. 254–264, 2009.

[23] MAEGE, I., JAEHNE, E., HENKE, A., et al., "Self-assembling adhesion promoters for corrosion resistant metal polymer interfaces", *Progress in Organic Coatings*, v. 34, n. 1-4, pp. 1-12, 1998.

[24] BARBOSA, L. C. A., "*Infrared spectroscopy for organic compounds characterization*", UFV ed, Viçosa, pp. 189, 2007 (In Portuguese).

[25] KOUISNI, L., AZZI, M., DALARD, F., et al., "Phosphate coatings on magnesium alloy AM60: Part 2: Electrochemical behaviour in borate buffer solution", *Surface and Coatings Technology*, v. 192, n. 2-3, pp.

239-246, 2005.

[26] BALTAT-BAZIA, A., CELATI, N., KEDDAM, M., et al., “Electrochemical Impedance Spectroscopy and microscopies applied to the structure of anodic layers on pure aluminum”, *Materials Science Forum*, v. 359, pp. 111-112, 1992.

[27] QUEIROZ, F.M., MAGNANI, M., COSTA, I., et al., “Investigation of the corrosion behaviour of AA 2024-T3 in low concentrated chloride media*”, Corrosion Science*, v. 50, n. 9, pp. 2646-2657, 2008.